Aerosol Science and Technology
Publication details, including instructions for authors and subscription information:
http://www.tandfonline.com/loi/uast20

Thermophoretic Deposition of Particles in Laminar and Turbulent Tube Flows

Chuen-Jinn Tsai [a] , Jyh-Shyan Lin [a] , Shankar G. Aggarwal [a] & Da-Ren Chen [b]
[a] Institute of Environmental Engineering, National Chiao Tung University , Hsin Chu, Taiwan
[b] Department of Mechanical Engineering, Joint Program in Environmental Engineering, University of Washington in St. Louis , St. Louis, Missouri, USA
Published online: 17 Aug 2010.

To cite this article: Chuen-Jinn Tsai , Jyh-Shyan Lin , Shankar G. Aggarwal & Da-Ren Chen (2004) Thermophoretic Deposition of Particles in Laminar and Turbulent Tube Flows, Aerosol Science and Technology, 38:2, 131-139, DOI: 10.1080/02786820490251358

To link to this article: http://dx.doi.org/10.1080/02786820490251358

Aerosol Science and Technology, 38:131–139, 2004

ISSN: 0278-6826 print / 1521-7388 online
DOI: 10.1080/02786820490251358

Thermophoretic Deposition of Particles in Laminar and Turbulent Tube Flows

Chuen-Jinn Tsai,[1] Jyh-Shyan Lin,[1] Shankar G. Aggarwal,[1] and Da-Ren Chen[2]
[1]*Institute of Environmental Engineering, National Chiao Tung University, Hsin Chu, Taiwan*
[2]*Department of Mechanical Engineering, Joint Program in Environmental Engineering, University of Washington in St. Louis, St. Louis, Missouri, USA*

Thermophoretic deposition of aerosol particles (particle diameter ranges from 0.038 to 0.498 μm) was measured in a tube (1.18 m long, 0.43 cm inner diameter, stainless steel tube) using monodisperse NaCl test particles under laminar and turbulent flow conditions. In the previous study by Romay et al., theoretical thermophoretic deposition efficiencies in turbulent flow regime do not agree well with the experimental data. In this study, particle deposition efficiencies due to other deposition mechanisms such as electrostatic deposition for particles in Boltzmann charge equilibrium and laminar and turbulent diffusions were carefully assessed so that the deposition due to thermophoresis alone could be measured accurately. As a result, the semiempirical equation developed by Lin and Tsai in laminar flow regime and the theoretical equation of Romay et al. in turbulent flow regime are found to fit the experimental data of thermophoretic deposition efficiency very well with the differences of less than 1.0% in both flow regimes. It is also found that Talbot's formula for the thermophoretic coefficient is accurate while Waldmann's free molecular formula is only applicable when Kn is greater than about 3.0.

INTRODUCTION

Thermophoresis is a phenomenon in which a temperature gradient in a gas causes suspended particles to migrate in the direction of decreasing temperature. Experimental and theoretical knowledge of thermophoresis is of great interest as it has various industrial and laboratory applications. Extensive experimental and theoretical/numerical work have been published on thermophoresis (Waldmann 1961; Derjaguin et al. 1976; Talbot et al. 1980), thermophoretic particle deposition in laminar tube/duct flow (Walker et al. 1979; Batchelor and Shen 1985; Stratmann and Fissan 1989; Montassier et al. 1990, 1991; Stratmann et al. 1994; Tsai and Lu 1995; He and Ahmadi 1998; Lin and Tsai 2003), thermophoretic particle deposition in turbulent tube/duct flow (Nishio et al. 1974; Shimada et al. 1994; Romay et al. 1998; He and Ahmadi 1998), the application of thermophortic force to suppress particle deposition on wafer surface (Stratmann et al. 1988; Bae et al. 1995), and enhancing particle deposition on impactor surface by thermophoresis (Lee and Kim 2002).

While most of the previous researches focused on the thermophoretic deposition in laminar flow regime seem to agree well with the experimental data, the study in turbulent tube flow by Romay et al. (1998) found that differences between their theoretical predictions and experimental data existed and increased with the flow Reynolds number. When the flow Reynolds number equaled 5517, the deviation was about 3%, and it increases to about 10% when the Reynolds number was increased to 9656. Similar discrepancy was found when the theoretical predictions of Romay et al. (1998) were compared with the experimental data of Nishio et al. (1974). Romay et al. argued that the discrepancy may be due to inertially enhanced thermophoresis for laminar flows over curved surfaces (Konstandopoulos and Rosner 1995) and enhanced thermophoreis caused by nonuniform concentration gradients and reverse thermophoresis in the preparation of heated aerosol source (Weinberg 1982). Therefore, it is worthwhile for this study to obtain more accurate particle deposition efficiency data to validate the theoretical equations of themophoretic deposition efficiency, in particular in turbulent flow regime. For validation purposes, the deposition efficiency in laminar flow regime was first measured and compared with the semiempirical equation developed by Lin and Tsai (2003).

In the experiment, other deposition mechanisms were also measured first by setting the wall temperature the same as gas flow temperature. In the actual thermophoretic deposition experiment, deposition efficiencies due to other mechanisms can then

Received 23 January 2003; accepted 22 August 2003.
The authors would like to thank the Taiwan National Science Council for the financial support of the project NSC 91-2211-E-009-008.
Address correspondence to Chuen-Jinn Tsai, Institute of Environmental Engineering, National Chiao Tung University, No. 75 Poai St., Hsin Chu, 300 Taiwan. E-mail: cjtsai@mail.nctu.edu.tw

Table 1
Theoretical expressions of the thermophoretic deposition efficiency in turbulent flow

Romay et al. (1998)	$\eta_{tur}(\%) = 100 \times \left\{1 - \left[\frac{T_w + (T_e - T_w)\exp(-\pi D_t h L/\rho Q C_p)}{T_{in}}\right]^{\Pr K_{th}}\right\}$
Nishio et al. (1974)	$\eta_{tur}(\%) = 100 \times \left\{1 - \exp\left(-\frac{\rho C_P K_{th} \nu (T_e - T_w)}{k_g \bar{T}}\left(1 - \exp\left(\frac{-4hL}{u_m \rho C_p D_t}\right)\right)\right)\right\}$

be assessed, and the deposition efficiency due to theromphoresis alone can be obtained accurately. Other deposition mechanisms include laminar diffusion and gravitational settling (Hinds 1999), particle electrostatic charges (Cohen 1995; Pich 1978; Ye et al. 1991), and turbulent diffusional and inertial deposition (Friedlander 2000; Lee and Gieseke 1994).

For submicron particles used in this study, gravitational settling is usually not important, while laminar diffusion and electrostatic deposition can be important. Cohen et al. (1995) passed monodisperse singly charged particles through a conducting copper tube and found that particle deposition efficiencies varied from 1 to 4% for particle diameter ranged from 0.015–0.095 μm at a mean flow rate of 4.6 l min^{-1} under laminar flow conditions. However the corresponding theoretical efficiencies by Pich (1978) were only from 0.04 to 0.11%, respectively. Ye et al. (1991) studied the electrostatic deposition efficiency of an annular denuder and found singly charged particles and particles in Boltzmann charge equilibrium had higher deposition efficiency than neutral particles. For example, for a 0.03 μm particle the deposition efficiencies for Boltzmann charge equilibrium condition and neutral condition are 12.6% and 2.4%, respectively, and for a 0.75 μm particle the deposition efficiencies are 4.0% and 1.5%, respectively. That is, even for conductor tubing and for particles that are in Boltzmann charge equilibrium, the deposition efficiency due to electrostatic is still important and must be measured carefully. Some previous investigators who used particles in Boltzmann charge equilibrium as test particles could obtain inaccurate deposition efficiency data for thermophoretic deposition efficiency. In this study, particles in both Boltzmann charge equilibrium and charge neutral conditions were used, and experimental data were compared to see if there were differences existed.

THERMOPHORETIC DEPOSITION EFFICIENCY IN LAMINAR AND TURBULENT TUBE FLOWS

In our previous study (Lin and Tsai 2003), the thermophoretic deposition efficiency for fully developed laminar tube flow is derived semiempirically as a function of the product of the Prandtl number and thermophoretic coefficient, i.e., $\Pr K_{th}$, and the dimensionless temperature $(T_e - T_w)/T_e$ as

$$\eta_{\ell am}(\%) = 78.3\left(\Pr K_{th}\frac{T_e - T_w}{T_w}\right)^{0.94}, \qquad [1]$$

where K_{th} is defined as (Talbot et al. 1980)

$$K_{th} = \frac{2C_s C}{(1 + 3C_m(2\lambda/d_p))} \times \left(\frac{k_g/k_p + C_t(2\lambda/d_p)}{1 + 2(k_g/k_p) + 2C_t(2\lambda/d_p)}\right). \qquad [2]$$

For turbulent tube flow, previous studies of Romay et al. (1998) and Nishio et al. (1974) have resulted in the theoretical expressions given in Table 1. In this study, both expressions were used to predict the thermophoretic deposition efficiency in turbulent tube flow.

EXPERIMENTAL METHOD

The experimental setup is shown in Figure 1. The experimental system consists of three parts: (1) the aerosol generation and conditioning section, which produces monodisperse aerosol with known diameter with a predetermined temperature; (2) the experimental section, which establishes a temperature gradient between the tube wall and gas; and (3) temperature, flow, and particle measurement systems, which measure the particle deposition efficiency at a certain flow rate and temperature gradient.

The aerosol was generated by a Collison atomizer and mixed with clean dry air in a mixing tank, and then passed through a silica gel diffusion dryer. After drying, the aerosol was neutralized by a TSI 3077 electrostatic charge neutralizer. After neutralization, the aerosol was passed through a differential mobility analyzer (DMA; TSI 3081 Long DMA column) where a high-voltage was applied to select particles of a known electrical mobility. The extracted monodisperse aerosol was neutralized again, and then mixed with clean dilution air in another mixing tank. To remove charged particles completely, an electrical condenser was used between the neutralizer and mixing tank so that the deposition efficiency of charge-neutral particles could be measured. In some experiments, the electrical condenser was not used and the deposition efficiency for particles in Boltzmann charge equilibrium was measured and compared with that of neutral particles.

In the conditioning section, the monodisperse aerosol stream was passed through a heat exchanger with a thermostated silicon-oil bath and was heated to a desired temperature. In the experimental section, the tube wall temperature was kept at 296 K by another heat exchanger with a thermostated water bath to establish a temperature gradient between the gas and wall of the tube in order to induce particle deposition by thermophoresis.

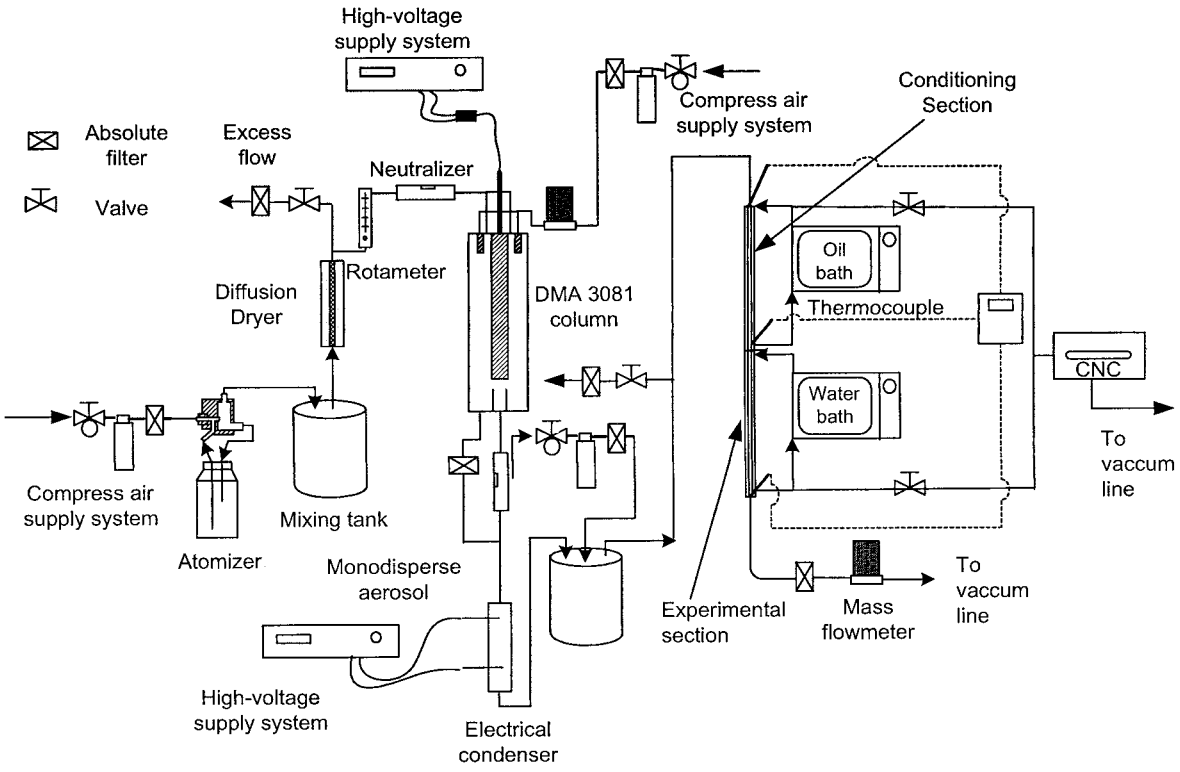

Figure 1. The schematic diagram of the experimental setup.

Three thermocouples—at the inlet of conditioning section, at the outlet of the experimental section, and at the junction between the conditioning section and experimental section—were installed to monitor the temperature at these points of the aerosol stream. The aerosol coming out from the experimental section was passed through a filter and then a mass flow-controlling device (MKS Instruments, Inc.) before it was exhausted into a vacuum line. The aerosol concentrations at the inlet and at the outlet of the experimental section were measured using a TSI 3760 clean room condensation nucleus counter (CNC), which had a sample flow rate of 1.5 l min^{-1}.

The particle material used in this study was NaCl. Normally 0.5% w/v aqueous solution of NaCl was used. The concentration was increased to about 1.5% for the larger particle sizes ($d_p > 0.35$ μm) investigated. The flow rate of sheath air and polydisperse aerosol stream of the DMA was kept constant, i.e., 5 and 0.5 l min^{-1}, respectively, throughout the experiment.

The experimental conditions are given in Table 2. During the experiment, the applied voltage was adjusted to get the particle of a desired diameter from the DMA. The flow rate in the experimental section was set using the downstream mass flow controller. The particle concentrations at the inlet and outlet of experimental section were measured by the CNC sequentially to determine the nonthermophoretic deposition efficiency. The deposition efficiency was first determined when no heating was applied in the conditioning section and gas temperature remained the same as tube wall temperature in the experimental section. This is to assess the deposition efficiency of other mechanisms, allowing an accurate determination of the thermophoretic deposition efficiency. For thermophoretic deposition measurements, the gas temperature at the conditioning section was heated to a desired value using the heat exchanger, while the temperature of the experimental section was kept constant (296 K) throughout this study. The particle concentrations at the inlet of the conditioning section and the outlet of experimental section were

Table 2
Experimental conditions

Parameter	Condition
Pressure at the inlet of the tube	1 atm
Airflow rate, l min^{-1}	4, 20, and 32
Inlet temperature, K	
Conditioning section	296–398
Experimental section	296
Voltage on the inner collector rod, volts	75–4800
Particle size, μm	0.038–0.498
Reynolds numbers	1340–10200
Tube length, m	2.74
Conditioning section	1.56
Experimental section	1.18
Tube inner diameter, cm	0.43
Particle material	NaCl

measured to determine the total deposition efficiency. After deducting deposition efficiencies due to other particle deposition mechanisms from the total deposition efficiencies, the experimental thermophoretic deposition efficiency can be obtained. During the measurement process, it was found that the nonthermophoretic deposition in the conditioning section could be suppressed completely when the tube wall temperature was heated higher than 343 K, which was the minimum temperature in the conditioning section. Therefore, it is not necessary to consider particle deposition losses in this section.

The above procedure was repeated for different flow rates and particle sizes. One data point at a particular test condition and particle size was the average of 6–8 efficiency measurements, while each measurement consisted of 10 particle concentration readings at the inlet and the outlet, respectively. The measurement time was about 2 min per 10 readings, excluding the system stabilization time, which was varied anywhere from 20–100 s/reading. After the completion of one efficiency measurement, the experimental section was cleaned by passing the clean air through it before the next measurement was started.

EXPERIMENTAL RESULTS AND DISCUSSION

Deposition Efficiency of Other Mechanisms

In laminar tube flow, particles may be deposited in the tube due to Brownian diffusion and electrostatic deposition. The experiment was done when both the aerosol stream and tube wall were kept at the same temperature, 296 K, in the laminar flow condition (4 l min^{-1}) so that there was no thermophoretic deposition. The theoretical diffusional deposition efficiencies are compared with the experimental data for charge-neutral particles and particles in Boltzmann charge equilibrium in Figure 2. The error bars in the figure indicate that the relative standard deviations of the data points are about ±20%. The diffusional deposition efficiency in laminar tube flow is the following (Hinds 1999):

$$\eta_{d,\ell} = 5.50\mu^{2/3} - 3.77\mu, \quad \text{for } \mu < 0.007, \qquad [3]$$

$$\eta_{d,\ell} = 1 - 0.819\exp(-11.5\mu) - 0.0975\exp(-70.1\mu), \quad \text{for } \mu \geq 0.007, \qquad [4]$$

where $\mu = DL/Q$, and $D = \text{KTB}$.

The results in Figure 2 show that the experimental data are about 2.2% higher than the theoretical diffusional deposition efficiencies for particles in Boltzmann charge equilibrium and when the particle diameter is less than 0.15 μm, and the deviation increases the decreasing particle size with the maximum of about 3.8% for 0.038 μm particles. For charge-neutral particles, the experimental data are very close to the theoretical diffusional deposition efficiencies, and the absolute differences are less than 0.65% for all particle sizes. That is, it is important to consider electrostatic deposition even for particles that are in Boltzmann charge equilibrium since the experimental thermophoretic deposition efficiencies are small, which are generally less than 10% in this study.

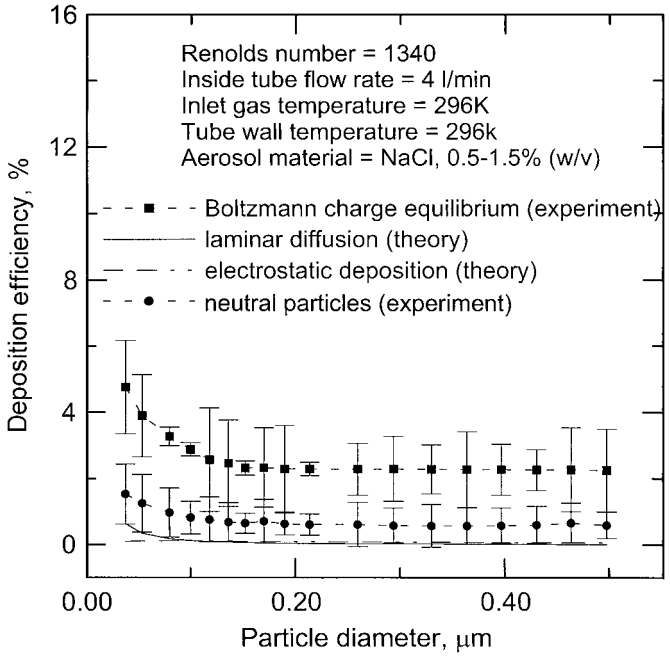

Figure 2. Comparison of experimental deposition efficiencies (nonthermophoretic) and theoretical predictions of diffusional and electrostatic deposition under laminar flow conditions (Re = 1340).

The electrostatic particle deposition efficiency is calculated as (Pich 1978)

$$\eta_e = (6\tau_e)^{1/3}, \qquad [5]$$

where

$$\tau_e = \frac{q^2 tC}{4\pi\varepsilon_0 Fr_0^3}, \qquad [6]$$

$$F = 3\pi\mu d_p. \qquad [7]$$

The electrostatic deposition efficiencies as a function of particle diameter for particles in Boltzmann charge equilibrium are also shown in Figure 2. It can be seen that the theoretical efficiency is indeed very small compared to the experimental data, and it warrants further theoretical study on the deposition due to particle electrostatic.

Particles deposition in turbulent tube flow may be due to eddy diffusion and turbulent inertial deposition. The particle deposition velocity towards the tube wall due to eddy diffusion is as follows (Friedlander 2000):

$$V_d = 0.0118\,\text{Re}^{7/8}\,\text{Sc}^{1/3}(D/D_t). \qquad [8]$$

To compute penetration efficiency due to eddy diffusion, one can use the following equation, which is based on the mass conservation principle, as

$$P_{d,t} = \exp(-\pi D_t V_d L/Q). \qquad [9]$$

Equation (8) indicates that small particles tend to have higher V_d and hence higher deposition efficiency. This is because small particles (less than 0.1 μm) follow eddy motion easily, resulting in an increase in the wall deposition rate. Large particles greater than 1.0 μm are unable to follow eddy motion smoothly and can be projected to the wall due to inertial force through the relatively quiescent fluid near the tube surface. This causes deposition rate of large particles to be increased. Such mechanism is called turbulent inertial deposition. The dimensionless particle deposition velocity of turbulent deposition developed by Friedlander and Johnstone (1957) is

$$\begin{aligned} V_d^+ &= V_d/u^* \\ &= \frac{1}{1883/(\tau^+)^2 - 50.6 + 1/\sqrt{f/2}}, \quad \text{for } 0.9\tau^+ \le 5, \\ &= \frac{1}{5\ln\frac{5.04}{0.9\tau^+/5-0.96} - 13.73 + 1/\sqrt{f/2}}, \\ &\qquad\qquad \text{for } 5 < 0.9\tau^+ \le 30, \\ &= \sqrt{f/2}, \quad \text{for } 0.9\tau^+ < 5. \end{aligned} \tag{10}$$

The penetration efficiency, P_{tur}, is computed using Equations (8)–(10). The particle deposition efficiency, including both eddy diffusion and turbulent deposition in turbulent tube flow, is calculated as

$$\eta_t = 1 - (P_{d,t} \times P_{tur}). \tag{11}$$

Figure 3 shows the comparison of theoretical results-based Equation (11) with experimental deposition efficiencies

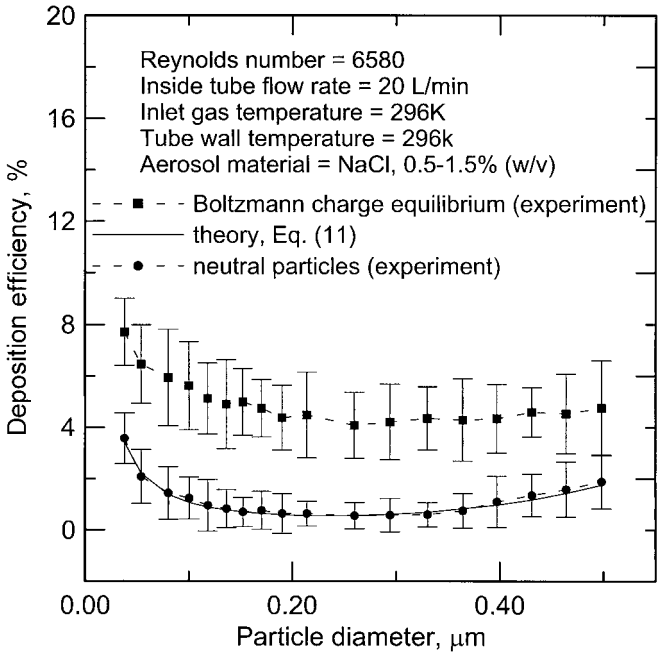

Figure 3. Comparison of experimental deposition efficiencies (nonthermophoretic) and theoretical predictions of combined turbulent diffusion and inertial deposition under turbulent flow conditions (Re = 6580).

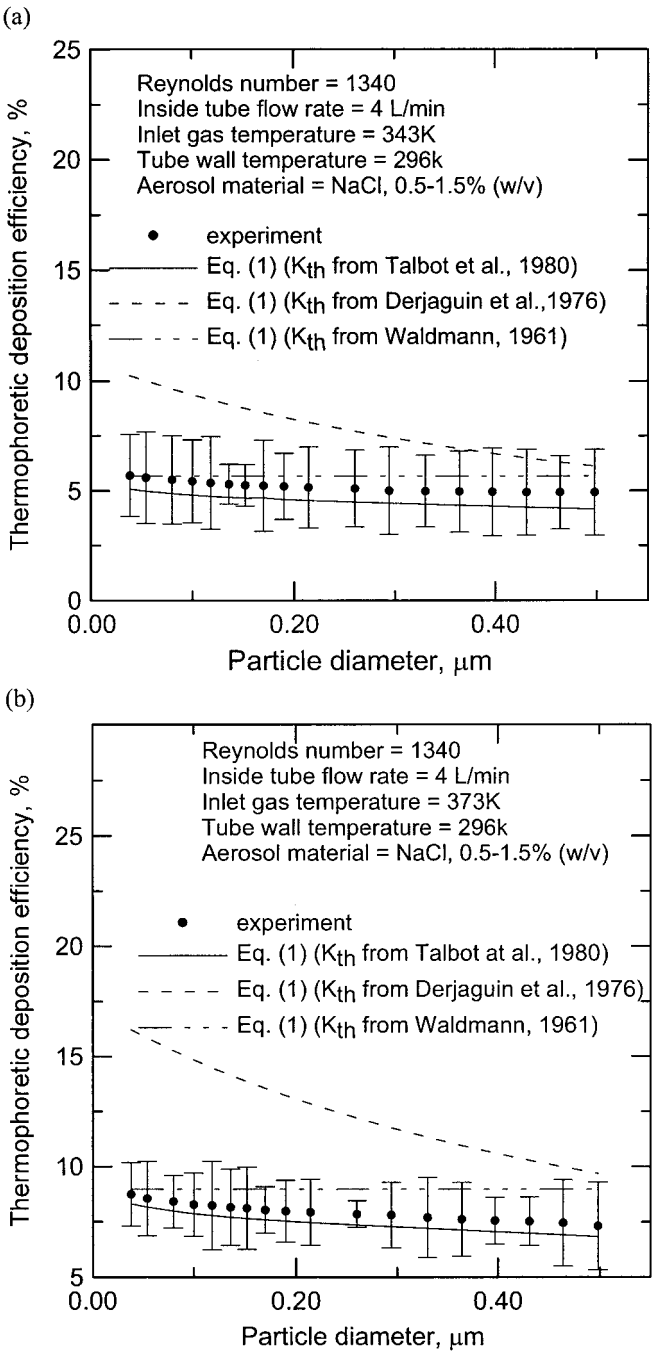

Figure 4. Comparison of experimental data and theoretical predictions of thermophoretic deposition efficiency of Lin and Tsai (2003) under laminar flow conditions: (a) Re = 1340, T_e = 343 K; (b) Re = 1340, T_e = 373 K.

(nonthermophoretic) with error bars indicated under turbulent flow (20 l min^{-1}) condition, for the particle diameter ranging 0.038–0.498 μm. The graph illustrates that the experimental efficiencies are about 3.5% higher than the theoretical efficiencies for particles in Boltzmann charge equilibrium. But for neutral particles, particle deposition efficiencies are lower and agree very well with the theoretical predictions. Again, the electrostatic deposition for particles in Boltzmann charge equilibrium is seen to be important and must be accounted for. It is best if one could use neutral particles for an accurate thermophoretic deposition experiment without the interference from electrostatic deposition. Also the calculation shows that the deposition due

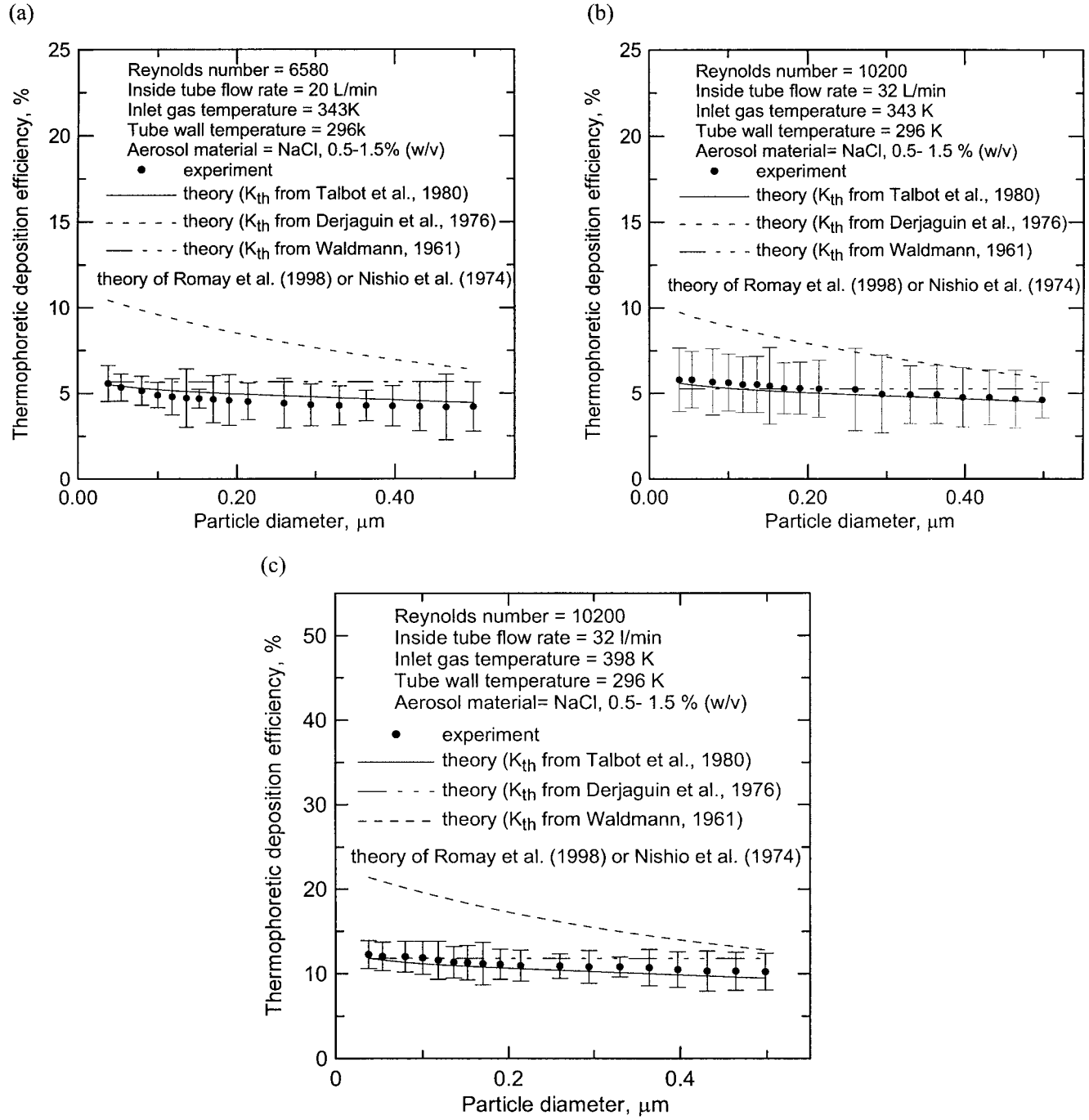

Figure 5. Comparison of experimental data and theoretical predictions of thermophoretic deposition efficiency of Romay et al. (1998) under turbulent flow conditions: (a) Re = 6580, T_e = 343 K; (b) Re = 10200, T_e = 343 K; (c) Re = 10200, T_e = 398 K.

to turbulent inertial deposition is much smaller than that due to eddy diffusion. The deposition efficiency due to turbulent inertial deposition increases only slightly from 0.0% for 0.038 μm particles with the increasing particle diameter to a maximum value of about 0.5% for the particle of 0.498 μm in diameter.

Thermophoretic Deposition Efficiency

Figures 4a and b show that in laminar flow condition experimental thermophoretic deposition efficiencies (with error bars) at 343 K and 373 K, after excluding other nonthermophoretic deposition efficiencies, are in good agreement with the theoretical predictions (Equation (1)) with the thermophoretic coefficient suggested by Talbot et al. (1980). The theoretical coefficient of Derjaguin et al. (1976) leads to the overestimation of the thermophoretic deposition efficiency in the range of particle sizes tested. Figures 4a and b also show that the thermophoretic deposition efficiency increases with an increasing inlet gas temperature. The theoretical efficiency based on the thermophoretic coefficient of Waldmann (1961) is nearly a horizontal line, indicating that it is independent of particle size. The theoretical predictions based on the coefficient of Waldmann are higher than the experimental data, and they agree only when the particle size is smaller than 0.038 μm.

In the turbulent flow regime, Figure 5a again shows that the experimental thermophoretic efficiencies (with error bars, at 343 K) are very close to the theoretical values based on the thermophoretic coefficient of Talbot et al. (1980) (flow rate equals 20 l min^{-1}). When the flow rate is increased further to 32 l min^{-1} (Figures 5b and c), the experimental thermophoretic deposition efficiencies are still in very good agreement with theoretical predictions based on the coefficient of Talbot et al. (1980), despite that the reading of the CNC becomes more fluctuating. Figure 5c shows that when inlet gas temperature is increased to 398 K the experimental thermophoretic deposition efficiency of this study is close to the theoretical prediction of

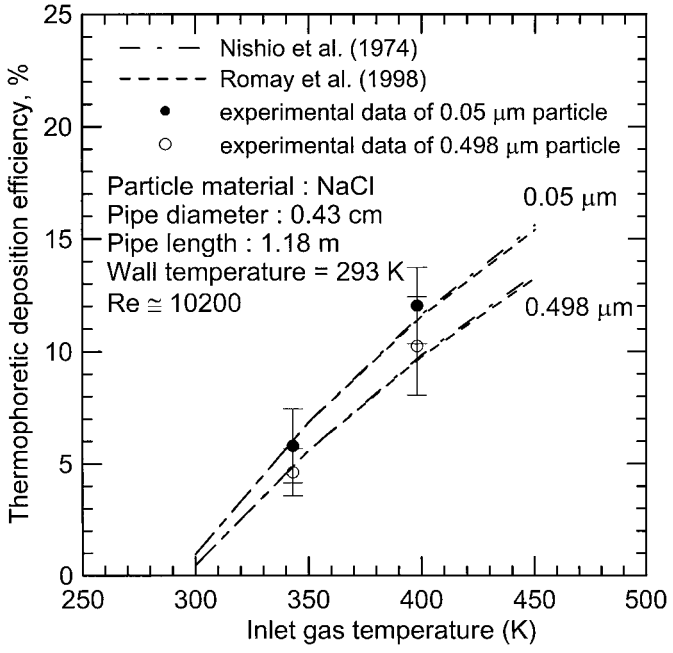

Figure 6. Comparison of theoretical predictions (Re = 10200) for particles of 0.05 and 0.498 μm in diameter in turbulent flow.

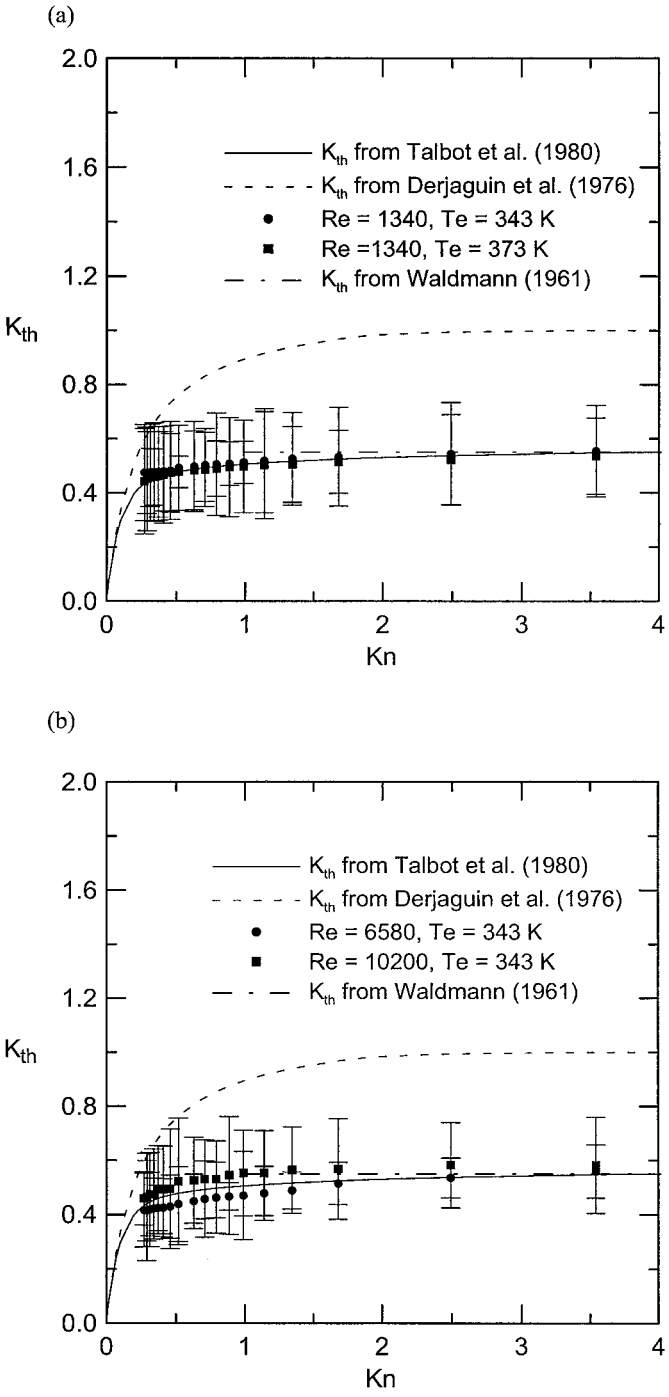

Figure 7. Comparison of experimental thermophoretic coefficients K_{th} with theories. Experimental K_{th} is calculated based on experimental data and theoretical thermophoretic deposition efficiency in (a) laminar flow and (b) turbulent flow.

Romay et al. (1998) after excluding other deposition mechanisms such as turbulent diffusion, inertial deposition, and particle electrostatic charge. The experimental data were again compared with the theoretical predictions of Romay et al. (1998) and Nishio et al. (1974) in Figure 6 for particles of 0.05 and 0.498 μm at Re = 10200. It can be seen that the experimental data agree very well with both theories.

In Figure 7a the thermoporetic coefficient derived from the experimental data of thermophoretic deposition efficiency is plotted as a function of the Knudsen number, $2\lambda/d_p$, in the laminar flow regime. It shows that the present experimental data agree well with the theory of Talbot et al. (1980). The relative standard deviations of the data points are less than $\pm 20\%$. The filled circles illustrate the experimental data of inlet gas temperature at 343 K and filled squares are the experimental data at 373 K in laminar flow conditions. The dashed horizontal line represents the constant value of K_{th}, 0.55, by Waldmann (1961) for the free molecular flow regime (Kn $\gg$ 1). The present data approach Waldmann's free molecular limit, as Kn is greater than about 3.0.

In the turbulent flow regime, Figure 7b also illustrates that the thermophoretic coefficient developed by Tablot et al. is much more accurate than that of Derjaguin et al. (1976) and Waldmann (1961). The relative standard deviation of the data points is less than $\pm 23\%$. It also indicates that Waldmann's thermophoretic coefficient is applicable when Kn greater than about 3.

CONCLUSIONS

In this study, thermophoretic particle deposition efficiencies in both laminar and turbulent tube flows were studied and compared with the theoretical expressions of Lin and Tsai (2003) and Romay et al. (1998), respectively. The experimental results show that the deposition efficiency due to particle diffusion and particle electrostatic charge is comparable to thermophoretic deposition efficiency and should be excluded so that one can obtain accurate experimental data for thermophoretic particle deposition efficiency. Even for particles in Boltzmann charge equilibrium, the deposition efficiency due to particle electrostatic charge is important when compared with the thermophoretic deposition efficiency. For particles that are completely charge neutral, the nonthermophoretic deposition efficiencies agree very with the available theories in the literature, while the thermophoretic deposition efficiencies also agree very well with the theoretical expressions of Romay et al. (1998) in turbulent flow and Lin and Tsai (2003) in laminar flow.

The present experimental data suggest that in both turbulent and laminar flows, Talbot's formula for the thermophoretic coefficient is accurate, while Waldmann's free molecular formula is only applicable when Kn is greater than about 3.0.

NOMENCLATURE

B	Dynamic mobility $B = C/3\pi\mu d_p$
C	slip correction factor
C_m	momentum exchange coefficient
C_s	thermal slip coefficient
C_t	temperature jump coefficient
d_p	diameter of the particle
D	particle diffusivity
D_t	Tube diameter
f	fanning friction factor
k_g	gas thermal conductivity
k_p	particle thermal conductivity
K	Boltzmann constant
K_{th}	thermophoretic coefficient
L	Tube length
$P_{d,\ell}$	diffusional penetration efficiency in laminar tube flow
$P_{d,t}$	diffusional penetration efficiency in turbulent tube flow
Pr	gas Prandtl number
P_{tur}	inertial deposition efficiency in turbulent tube flow
Re	Reynolds number
q	the charge on the particle
Q	Inlet gas flow rate
Sc	Schmidt number
t	the elapsed time in the tube
$\bar{T}$	average temperature of the fluid
T_e	gas temperature at inlet
T_w	wall temperature
u^*	Friction velocity $u^* = u_m\sqrt{(f/2)}$
u_m	Average gas velocity
V_d	Particle deposition velocity
z_{dep}	Thermal entry length

Greek Letters

β	thermophoretic parameter (in laminar tube flow) $\beta_1 = \mathrm{Pr}K_{th}(T_e - T_w)/T_w$
ε_0	the permittivity of air
η_e	electrostatic deposition efficiency
η_ℓ	nonthermophoretic deposition efficiency in laminar tube flow
$\eta_{\ell am}$	thermophoretic deposition efficiency in laminar tube flow
η_t	nonthermophoretic deposition efficiency in turbulent tube flow
η_{tur}	thermophoretic deposition efficiency in turbulent tube flow
λ	mean free path of air
μ	air dynamic viscosity
ν	air kinematic viscosity
ρ	gas density
ρ_p	particle density
τ	particle relation time $\tau = \rho_p d_p^2 C/18\mu$
τ^+	dimensionless particle relation time $\tau^+ = u^{*2}/\nu$

REFERENCES

Bae, G. N., Lee, C. S., and Park, S. O. (1995). Measurements and Control of Particle Deposition Velocity on a Horizontal Wafer with Thermophoretic Effect, *Aerosol Sci. Technol.* 23:321–330.

Batchelor, G. K., and Shen, C. (1985). Thermophoretic Deposition of Particles in Gas Flowing Over Cold Surfaces, *J. Colloid Interface Sci.* 107:21–37.

Cohen, B. S., Xiong, J. Q., Asgharian, B., and Ayres, L. (1995). Deposition of Inhaled Charged Ultrafine Particles in a Simple Tracheal Model, *J. Aerosol Sci.* 26:1149–1160.

Derjaguin, B. V., Rabinovich, Ya. I., Storozhilova, A. I., and Scherbina, G. I. (1976). Measurement of the Coefficient of Thermal Slip of Gases and the Thermophoresis Velocity of Large-Size Aerosol Particles, *J. Colloid Interface Sci.* 57:451–461.

Friedlander, S. K., and Johnstone, H. F. (1957). Deposition of Suspended Particles from Turbulent Gas Stream, *Ind. Engr. Chem.* 49:1151–1156.

Friedlander, S. K. (2000). *Smoke, Dust, and Haze*, John Wiley & Sons, New York.

He, C., and Ahmadi, G. (1998). Particle Deposition with Thermophoresis in Laminar and Turbulent Duct Flows, *Aerosol Sci. Technol.* 29:525–546.

Hinds, W. C. (1999). *Aerosol Technology*, 2nd ed. Wiley, New York.

Kays, W. M., and Crawford, M. E. (1993). *Convective Heat and Mass Transfer*, 3rd ed., McGraw-Hill, New York.

Konstandopoulos, A., and Rosner, D. E. (1995). Inertial Effects on Thermophoretic Transport of Small Particles to Walls with Streamwise Curvature—I. Theory, *Int. J. Heat Mass Transfer* 38:2305–2327.

Lee, B. U., and Kim, S. S. (2002). The Effect of Varying Impaction Plate Temperature on Impactor Performance: Experimental Results, *J. Aerosol Sci.* 33:451–457.

Lee, K. W., and Gieseke, J. A. (1994). Deposition of Particles in Turbulent Pipe Flows, *J. Aerosol Sci.* 25:699–709.

Lin, J.-S., and Tsai, C.-J. (2003). Thermophoretic Deposition Efficiency in a Cylindrical Tube Taking into Account Developing Flow at the Entrance Region, *J. Aerosol Sci.* 34:569—583.

Montassier, N., Boulaud, D., and Renoux, A. (1991). Experimental Study of Thermophoretic Particle Deposition in Laminar Tube Flow, *J. Aerosol Sci.* 22:677–687.

Montassier, N., Boulaud, D., Stratmann, F., and Fissan, H. (1990). Comparison Between Experimental Study and Theoretical Model of Thermophoretic Particle Deposition in Laminar Tube Flow, *J. Aerosol Sci.* 21:S85–S88.

Nishio, G., Kitani, S., and Takahashi, K. (1974). Thermophoretic Deposition of Aerosol Particles in a Heat-Exchanger Pipe, *Ind. Engng. Chem. Process Des. Develop.* 13:408–415.

Pich, J. (1978). Comments on the Paper: C. P. Yu's Precipitation of Unipolarly Charged Particles in Cylindrical and Spherical Vessels, *J. Aerosol Sci.* 9:275–278.

Romay, F. J., Takagaki, S. S., Pui, D. Y. H., and Liu, B. Y. H. (1998). Thermophoretic Deposition of Aerosol Particles in Turbulent Pipe Flow, *J. Aerosol Sci.* 29:943–959.

Shimada, M., Seto, T., and Okuyama, K. (1994). Wall Deposition of Ultrafine Aerosol Particles by Thermophoresis in Nonisothermal Laminar Pipe Flow of Different Carrier Gas, *Jpn. J. Appl. Phys.* 33:1174–1181.

Stratmann, F., and Fissan, H. (1989). Experimental and Theoretical Study of Submicron Particle Transport in Cooled Laminar Tube Flow Due to Combined Convection, Diffusion and Thermophoresis, *J. Aerosol Sci.* 20:899–902.

Stratmann, F., Otto, E., and Fissan, H. (1994). Thermophoretic and Diffusional Particle Transport in Cooled Laminar Tube Flow, *J. Aerosol Sci.* 25:1305–1319.

Stratmann, F., Fissan, H., Papperger, A., and Friedlander, S. (1988). Suppression of Particle Deposition to Surfaces by the Thermophoretic Force, *Aerosol Sci. Technol.* 9:115–121.

Talbot, L., Cheng, R. K., Schefer, R. W., and Willis, D. R. (1980). Thermophoresis of Particles in a Heated Boundary Layer, *J. Fluid Mech.* 101:737–758.

Tsai, C.-J., and Lu, H.-C. (1995). Design and Evaluation of a Plate-to-Plate Thermophoretic Precipitator, *Aerosol Sci. Technol.* 22:172–180.

Waldmann, L. (1961). In *Rarefiled Gas Dynamics*, edited by L. Talbot. Academic, New York, p. 323.

Walker, K. L., Homsy, G. M., and Geyling, R. T. (1979). Thermophoretic Deposition of Small Particles in Laminar Tube Flow, *J. Colloid Interface Sci.* 69:138–147.

Weinberg, M. C. (1982). Thermophoretic Deposition Efficiency for a Nonuniform Inlet Particle Concentration, *J. Amer. Ceramic Soc.* 65:638–641.

Ye, Y., Tsai, C. J., and Pui, D. Y. H. (1991). Particle Transmission Characteristics of an Annular Denuder Ambient Sampling System, *Aerosol Sci. Technol.* 14:102–111.